

Non-trivial Behavior of Temperature of Dielectric Constant Maximum in (Pb/La)(Zr/Ti)O₃ 9/65/35 Relaxor Ferroelectric Ceramics Detected by Acoustic Emission

Evgeniy Dul'kin^{a*}, Michael Roth^a, Floriana Craciun^b, Carmen Galassi^c

^aThe Hebrew University of Jerusalem, Department of Applied Physics, 91904, Jerusalem, Israel.

^bIstituto di Struttura della Materia, Area della Ricerca di Tor Vergata, 00133, Rome, Italy.

^cIstituto di Scienza e Tecnologia dei Materiali Ceramici, 48018, Faenza, Italy.

Received: February 07, 2022; Revised: July 14, 2022; Accepted: August 1, 2022

9/65/35 PLZT relaxor was studied under a bias electric field using the acoustic emission method. It was established that the temperature of smeared dielectric constant maximum exhibits the V-shape, lying fully within the ergodic phase, as well as that the threshold electric field is found to be approximately the same as in both PMN-0.24PT and PFN-0.02PT relaxors. A reason of the latter phenomena is discussed from the viewpoint of incorporated ions properties.

Keywords: Relaxor ferroelectrics, Curie temperature, polar nanoregions, random electric fields, acoustic emission.

1. Introduction

During last twenty years the non-trivial behavior of temperature of smeared dielectric constant, ϵ' , maximum, T_m , induced by *dc* bias electric field, E , was recognized to be an intrinsic feature of the relaxor ferroelectrics, RFEs, like PMN, along with its frequency dependence. This non-trivial behavior of T_m , or V-shape effect, is that the T_m remains practically the same or even decreases as E enhances up to a certain threshold E_{th} , above which T_m increases and gradually tends to saturation¹.

The polar nanoregions, PNRs, characteristic for RFEs and absent in ferroelectrics, FEs, are the reason of the V-shape effect. For example in PMN, while arising due to Pb²⁺ ions off-centered shift, PNRs are initially pinned to random electric fields, RFs, in turn arising due to difference in B-sites ions charges². When applying E the PNRs start to switch along E causing the decrease of T_m . As E attains E_{th} , all the PNRs orient along E and T_m becomes minimum. As E further enhances the RFEs behave as the FEs and the T_m increases similar to Curie temperature, T_c , in dependence on E ¹.

An appearance of V-shape is well documented in pure canonical RFE of PMN and its non-canonical solution with FE of PbTiO₃, PMN-*x*PT². On cooling the PNRs cause maximum of ϵ' in T_m and then freeze in glass phase below freezing temperature, T_f , transforming the RFE from ergodic phase, ER, to non-ergodic, NER, one. When applying E the PMN remains in NER phase until the E enhances up to critical value, E_c , and then transforms to FE phase, T_f transforms to T_c and PNRs transform to macroscopic domains.

The behavior of both T_m and T_c in dependence on E , $T-E$ phase diagram, was studied well enough in both PMN and PMN-*x*PT^{1,3,4}. While T_m dependence exhibits a V-shape, T_c exhibits a quasi-linear dependence on E ³. The $T_c(E)$ quasi-linear curve separates the FE phase from the ER one, whereas

the $T_m(E)$ V-shape lies within the ER one when $E < E_{th}$. Both $T_m(E)$ and $T_c(E)$ dependences merge near E_{th} in a single line separating the FE and ER phases when $E > E_{th}$. It is need to stress that the piezomodule maximum occurs in the vicinity of V-shape³, that might be used in applications. Meanwhile, recently it was shown that the $T_m(E)$ V-shape fully lies within the ER phase in 0.70PMN-0.30PT crystals when applying the acoustic emission (AE)⁵. This is due to sharp bursts of AE in comparison with smeared dielectric maximum.

Besides, the $T-E$ phase diagram was thoroughly studied in Pb_{1-x}La_x(Zr_yTi_{1-y})_{1-x/4}O₃ with $x=0.09$ and $y=0.65$, denoted as 9/65/35 PLZT, ceramics⁶. This compound is similar to pure canonical PMN one: the NER phase exists up to $E_c \approx 4.8$ kV/cm, above which the FE phase forms (Figure 1). The $T_c(E)$ quasi-linear curve separates the FE phase from the ER one, too, but the $T_m(E)$ V-shape was not studied at all.

The goal of the present work is to study the dependence $T_m(E)$ to establish whether the T_m V-shape exists in 9/65/35 PLZT due to its importance for applications and, if yes, to compare it with those observed in other RFEs.

2. Experimental Details

The 9/65/35 PLZT ceramic samples were prepared via the conventional solid-state route, according to the formula Pb_{1-x}La_x(Zr_yTi_{1-y})_{1-x/4}O₃, which provides charge-compensating vacancies (for the Pb²⁺/La³⁺ substitution) in the Zr/Ti sublattice. The specific composition was Pb_{0.91}La_{0.09}(Zr_{0.65}Ti_{0.35})_{0.9775}Δ_{0.0225}O₃, where Δ represents B-site vacancies. Analytical-grade starting oxide powders were thoroughly mixed by ball-milling and calcined at 850°C for 4h, then sintered in two stages: at 1200 °C for 2h and at 1300°C, while packed with PbZrO₃+5 wt% excess ZrO₂ powder in alumina crucibles in order to maintain a constant PbO activity at the sintering temperature. The process was optimized to achieve samples with high density, high purity phase and good crystallization. The density was 97%

*e-mail: evgeniy.dulkin@mail.huji.ac.il

of the nominal value. A pure perovskite cubic structure was evidenced from x-ray diffraction spectra, with the unit cell size of 4.093 Å. Cross-section scanning electron microscopy evidenced a rather uniform microstructure with an average crystallite size of about 3.3 μm (Figure 2).

Samples with sizes of 4x4x0.45 mm³ cut from the same batch and annealed at 750°C for 30 min were used in the present work.

The AE technique is described in basic details elsewhere⁷. A ceramic plate sample with silver contacts is pasted with a silver epoxy to the polished side of a fused silica acoustic rod waveguide. A PZT-19 disk piezoelectric sensor is attached to the rear end of the waveguide. The sensor is electrically coupled to a 500 kHz band-pass low noise variable (up to 40 dB) preamplifier connected to a detector-amplifier (40 dB). A chromel-alumel thermocouple junction is glued to the waveguide near the sample by a special thermoconductor paste. The higher part of the acoustic waveguide with the pasted sample is mounted from below in a resistance element tube furnace.

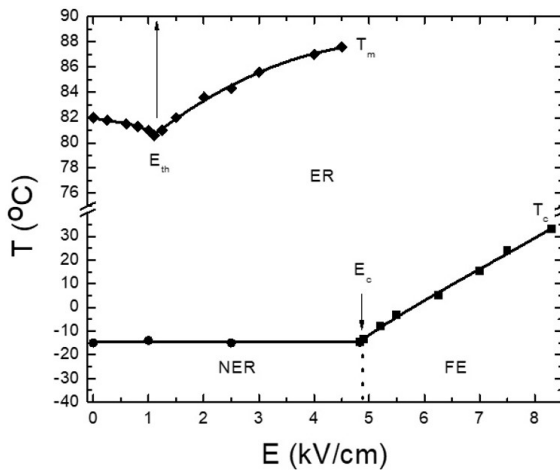


Figure 1. A plot of the T - E phase diagram of 9/65/35 PLZT ceramics: constructed from Ref. ⁶ (lower curve) and detected in the present work (higher curve).

The dielectric data are measured using a HP4263A LCR meter wired to the sample. The thermocouple, amplifier, and LCR meter outputs are interfaced with a PC for coupled readout. The measurement of both real part ϵ' of the dielectric constant and the AE count rate, \dot{N} (s⁻¹), are performed with the frequency of 10 kHz in the temperature range 50-125°C with a rate of about 1-3°C/min. When measuring the AE under a bias electric field E , a high voltage supply is wired to the sample along with ac electric field of 1 V in amplitude and the data are recorded by a fixed steps of E up to 5 kV/cm during the thermal cycling.

Before each cycle the sample is annealed at temperature of 125°C for 15 min and then measurements of both dielectric and AE data during cooling and heating under bias electric field, E (field heating after field cooling regime (FH-FC)), are performed.

3. Result and Discussion

Figure 3 presents the plot of real part of dielectric constant, ϵ' , in dependence on temperature, T , in absence of bias electric field, E . ϵ' exhibits a smeared maximum, characteristic for RFEs, and attains the value of about $6 \cdot 10^3$ at T_m in good agreement with that measured in Ref⁸. The sharp bursts of \dot{N} of AE point out the value of $T_m \approx 82.6^\circ\text{C}$ precisely enough in good agreement with that measured in Ref⁸, too, using the dielectric method. Because the 9/65/35 PLZT belongs to canonical RFEs, no thermal hysteresis is detected in T_m due to absence of any phase transition because ϵ' maximum is caused by the interactions between the PNRs only, causing the sharp bursts of \dot{N} similar to that detected in canonical RFEs $\text{Pb}(\text{Mg}_{1/3}\text{Ta}_{2/3})\text{O}_3$ ⁹.

Figure 1 presents the T - E phase diagram of behavior of T_m in 9/65/35 PLZT as well as the behavior of T_c in the same compound reconstructed from Ref⁶. It is clearly seen that the T_m , detected by AE, in dependence on E exhibits a V-shape, as it would be expected, lying fully within ER phrase as previously observed in PMN-0.30PT⁵. The E_{th} is found to be 1.15 kV/cm, that is approximately the same as in both PMN-0.24PT¹ and PFN-0.02PT¹⁰. Because the E_{th} is equivalent to RFs in the RFEs, it means that the 0.09 mol. of La^{3+} ions in 9/65/35 PLZT creates the same strength of

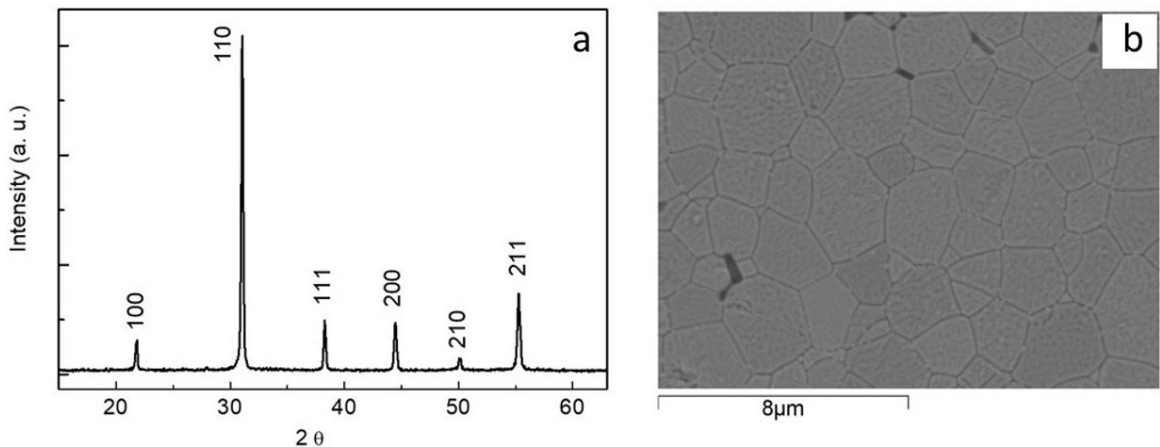


Figure 2. The XRD diffraction spectra (a), and cross-section SEM image (b) of 9/65/35 PLZT ceramics.

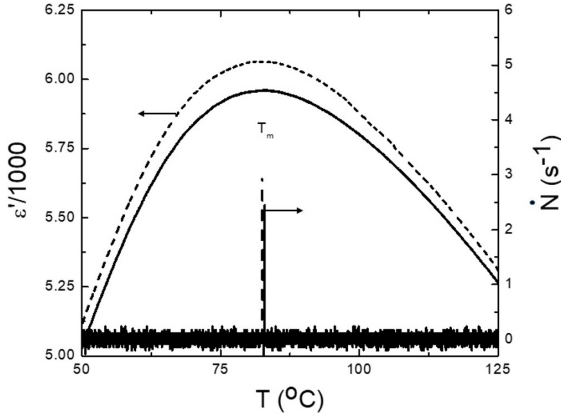


Figure 3. A plot of the real part ϵ' of the dielectric constant and the AE count rate, \dot{N} (s^{-1}), of 9/65/35 PLZT ceramics.

Table 1. Comparison of the E_{th} s in PMN- x PT and x /65/35 PLZT relaxor ferroelectrics.

Compound	x	Substituted site	E_{th} (kV/cm)	Source
PMN- x PT	0.24	B	1.12	[1]
PFN- x PT	0.02	B	~ 1	[10]
x /65/35 PLZT	0.09	A	1.15	Present

RFs that the 0.24 mol. of Ti^{4+} ions in PMN-0.24PT and the 0.02 mol. of Ti^{4+} ions in PFN-0.02PT (Table 1).

It is well known that in some RFEs an incorporation of the dopants essentially influences on RFs strength due to their differences in valences in comparison with hosting ions¹¹. Let us now consider the mechanisms of RFs creation in both x /65/35 PLZT and PMN- x PT and PFN- x PT compounds. In both PMN- x PT and PFN- x PT the Ti^{4+} ions substitute the Nb^{5+} ions in B^{''}-sites due to practical equality of their radii ($r_{Ti} = 0.605\text{\AA}$, $r_{Nb} = 0.64\text{\AA}$), that weakens the RFs strengths. No other mechanisms exist to influence the RFs strengths in both PMN- x PT and PFN- x PT when substituting the B-sites ions. The equality of RFs strengths created by 0.24 and 0.02 mol. of Ti^{4+} in both PMN- x PT and PFN- x PT is obviously caused by difference in valences of Mg^{2+} versus Fe^{3+} in their B[']-sites, respectively.

In x /65/35 PLZT, La^{3+} ions substitute Pb^{2+} ions in A-sites due to approximate equality of their radii ($r_{La} = 1.36\text{\AA}$, $r_{Pb} = 1.49\text{\AA}$), that enhances the RFs strengths. On the other hand, substitution of Pb^{2+} ions for La^{3+} ions is accompanied by arising of both A- and B-sites charge-compensating vacancies¹², which are another source of RFs that enhances the RFs summary strengths additionally. Also an incorporation of La^{3+} , possessing the isotropic outermost electron shell, disturbs the stereochemically active lone-pair electron shell of Pb^{2+} that leads to arising the corresponding electrostrictive strains similar to those detected using *in situ* Raman spectroscopy in $Pb_{1-x}La_xSc_{(1+x)/2}Ta_{(1-x)/2}O_3$ relaxor ferroelectric crystals¹³, which in turn create the weak RFs. So there are three mechanisms which influence the RFs strengths in x /65/35 PLZT.

Thus, we have concluded that the substitution of Pb^{2+} ions for La^{3+} ions in 9/65/35 PLZT creates the same strength of RFs that the substitution of Nb^{5+} ions for Ti^{4+} ions creates in

both PMN-0.24PT and PFN-0.02PT due to three mechanisms existing in x /65/35 PLZT instead of single mechanism in both PMN- x PT and PFN- x PT compounds.

4. Conclusion

In summary, we have studied the 9/65/35 PLZT ceramics under a bias electric field using the acoustic emission method. We have plotted the T - E phase diagram and established that the temperature of smeared dielectric constant maximum exhibits the V-shape, lying fully within the ergodic phase. We have measured the threshold field to be 1.15 kV/cm that is approximately the same that in both PMN-0.24PT and PFN-0.02PT. We have concluded that the 0.09 mol. of La^{3+} ions in 9/65/35 PLZT creates the same strength of random electric fields that the 0.24 and 0.02 mol. of Ti^{4+} ions creates in both PMN-0.24PT and PFN-0.02PT due to three mechanisms existing in 9/65/35 PLZT instead of single mechanism in both PMN-0.24PT and PFN-0.02PT.

5. References

- Raevski IP, Prosandeev SA, Emelyanov SM, Raevskaya SI, Colla EV, Viehland D, et al. Bias-field effect on the temperature anomalies of dielectric permittivity in $PbMg_{1/3}Nb_{2/3}O_3$ - $PbTiO_3$ single crystals. *Phys Rev B Condens Matter Mater Phys.* 2005;72(18):184104.
- Kleemann W. Random fields in relaxor ferroelectrics: a jubilee review. *J Adv Dielectr.* 2012;2(2):1241001.
- Raevskaya SI, Emelyanov SM, Savenko FI, Panchelyuga MS, Raevski IP, Prosandeev SA, et al. Quasivertical line in the phase diagram of single crystals of $PbMg_{1/3}Nb_{2/3}O_3$ - $xPbTiO_3$ ($x=0.00, 0.06, 0.13$, and 0.24) with a giant piezoelectric effect. *Phys Rev B Condens Matter Mater Phys.* 2007;76(6):060101.
- Dul'kin E, Mojaev E, Roth M, Raevski IP, Prosandeev SA. Nature of thermally stimulated acoustic emission from $PbMg_{1/3}Nb_{2/3}O_3$ - $PbTiO_3$ solid solutions. *Appl Phys Lett.* 2009;94(25):252904.
- Dul'kin E, Kania A, Roth M. On the question of the critical end point in the $(1-x)PbMg_{1/3}Nb_{2/3}O_3$ - $xPbTiO_3$ relaxor ferroelectric single crystals based on acoustic emission data studies. *Europhys Lett.* 2021;133(6):67001.
- Bobnar V, Kutnjak Z, Piric R, Levstik A. Electric-field-temperature phase diagram of the relaxor ferroelectric lanthanum-modified lead zirconate titanate. *Phys Rev B Condens Matter.* 1999;60(9):6420-7.
- Dul'kin E, Mojaev E, Roth M, Kamba S, Vilarinho PM. Burns, Néel, and structural phase transitions in multiferroic $Pb(Fe_{2/3}W_{1/3})O_3$ - $xPbTiO_3$ detected by an acoustic emission. *J Appl Phys.* 2008;103(8):083542.
- Craciun F. Strong variation of electrostrictive coupling near an intermediate temperature of relaxor ferroelectrics. *Phys Rev B Condens Matter Mater Phys.* 2010;81(18):184111.
- Dul'kin E, Kania A, Roth M. Detecting depinning of polar nanoregions under dc external electric field in canonical relaxor ferroelectric $Pb(Mg_{1/3}Ta_{2/3})O_3$ via acoustic emission. *Phys Status Solidi, B Basic Res.* 2016;253(10):1937-40.
- Sitalo EI, Zakharov YN, Lutokhin AG, Raevskaya SI, Raevski IP, Panchelyuga MS, et al. Bias field effect on dielectric and pyroelectric properties of $(1-x)Pb(Fe_{1/2}Nb_{1/2})O_3$ - $xPbTiO_3$ ceramics. *Ferroelectrics.* 2009;389(1):107-13.
- Dul'kin E, Roth M. Comparison of random field strengths in $(1-x)SrTiO_3$ - $xBiFeO_3$ and $(1-x)SrTiO_3$ - $xBaTiO_3$ relaxor ferroelectrics by means of acoustic emission. *Eur Phys J Appl Phys.* 2020;92(2):20401.
- Hardtl KH, Hennings D. Distribution of A-site and B-site vacancies in $(Pb,La)(Ti,Zr)O_3$ ceramics. *J Am Ceram Soc.* 1972;55(5):230-1.
- Maier BJ, Welsch A-M, Mihailova B, Angel RJ, Zhao J, Paulmann C, et al. Effect of La doping on the ferroic order in Pb-based perovskite-type relaxor ferroelectrics. *Phys Rev B Condens Matter Mater Phys.* 2011;83(13):134106.